Gabriela Tatiana Castro, Mauricio Andrés Filippa, Cecilia Mariana Peralta, María Virginia Davin, María Cristina Almandoz and Estela Isabel Gasull*

# Solubility and Preferential Solvation of Piroxicam in Neat Solvents and Binary Systems

https://doi.org/10.1515/zpch-2017-0946
Received February 22, 2017; accepted July 21, 2017

**Abstract:** The solubilization and solvatochromic behavior of piroxicam (PRX) were analyzed using UV-vis spectroscopy in neat (protic and aprotic) and binary solvent mixtures. The effects of solvent dipolarity/polarizability and solvent–solute hydrogen bonding interactions on the absorption maxima were evaluated by means of the linear solvation energy relationship concept of Kamlet and Taft. This analysis indicated that both interactions play an important role in the position of the absorption maxima in neat solvents. While, the PRX solubility depends on the solute–solvent specific interactions, polarizability and the cohesive forces of the solvent, manifested mainly by means of the Hildebrand's solubility parameter. Preferential solvation (PS) was studied in 10 binary mixtures. A non-ideal behavior of the wavenumber curve as the function of analytical mole fraction of co-solvent was detected. Index of preferential solvation, as well as the influence of solvent parameters were calculated. The process of dissolution was analyzed in aqueous binary mixtures of ethanol, ethylene glycol and propylene glycol. They were not spontaneous in all proportions, but when water concentration decreases in the mixtures, the process becomes more spontaneous.

**Keywords:** binary mixtures; piroxicam; preferential solvation; solvatochromism.

***Corresponding author: Estela Isabel Gasull,** Project PROICO 2-1614, Facultad de Química, Bioquímica y Farmacia, Universidad Nacional de San Luis, Chacabuco 917, D5700HHW, San Luis, Argentina, e-mail: esgasu@unsl.edu.ar
**Gabriela Tatiana Castro, Mauricio Andrés Filippa, Cecilia Mariana Peralta, María Virginia Davin and María Cristina Almandoz:** Project PROICO 2-1614, Facultad de Química, Bioquímica y Farmacia, Universidad Nacional de San Luis, Chacabuco 917, D5700HHW, San Luis, Argentina

# 1 Introduction

Piroxicam (PRX, 4-Hydroxy-2-methyl-N-2-pyridinyl-2H-l,2-benzothiazino-3-3-carboxamide-l,l-dioxide, Figure 1) is a member of non-steroidal anti-inflammatory drugs (NSAIDs) of the oxicam class. It is applied to mitigate the symptoms of rheumatoid and osteoarthritis, primary dysmenorrhoea, and postoperative pain, and act as an analgesic, mainly where there is an inflammatory component. Its anti-inflammatory effects are associated with reversible inhibition of cyclooxygenases COX-1 and COX-2, which results in the inhibition of the synthesis of prostaglandin and other inflammation mediators [1].

Solubility plays a critical role in various issues related to drug dissolution, absorption, and formulation development and production process as well as stability. Appropriate solubility and solvent system are required to develop formulations. Solubility is extensively utilized in crystallization and purification of active pharmaceutical ingredients and/or their intermediates. Also, solubility plays an important role in controlling the solid forms as well as the yields. Thus, finding a method to predict the solubility is very significant because it would allow optimizing several design processes. Previous studies have found that the aqueous solubility of PRX is poor [2]. To solve this problem, several methods have been used, such as: (i) the inclusion complexes of PRX with cyclodextrins [3, 4]; in this, the complexation occurs via several routes such as dissolution-solvent evaporation, co-precipitation, kneeding method and others [5]; (ii) the employ of different carriers in solid dispersion technique [6]; (iii) cosolvency using different alcohols [7–9]; (iv) sonication during the homogenization of a solid dispersion [10]; (v) the use of appropriate excipients such as polyvinylpyrrolidone [11], polyethylene glycols 4000 and 6000 [12], gelucire [13], among others.

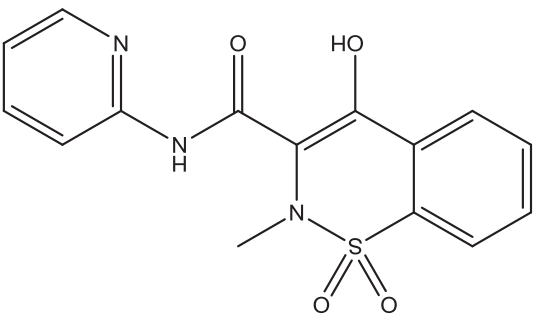


**Fig. 1:** Chemical structure of PRX.

To develop the solution chemistry is necessary the study of solvent influences on the structure and spectroscopic behavior of a solute [14–16]. The existence of specific and non-specific interaction between the solvent and the solute molecules are responsible, among other, for the change in the molecular geometry, electronic structure and dipolar moment of the solute. These solute–solvent interactions concern the solute's electronic absorption and emission spectra and this phenomenon is regarded as solvatochromism [17]. In addition, physicochemical properties, such as the rate, position of the equilibrium of processes as well as the p$K_a$ values are depending on the characteristics of the solvents in which they are carried out [18, 19]. Despite the importance of knowing the behavior of PRX in different solvent systems, no detailed studies are in the literature for this compound, to the best of our knowledge. Therefore, a detailed study of the solvation of this compound, which can influence its solubility and bioavailability, is important and necessary.

In previous reports the solubility of NSAIDs: ibuprofen, ketoprofen and naproxen in organic solvents and aqueous binary mixtures [20–22] and, on the other hand, the solvatochromic characteristics of sulfamethozaxole, trimethoprim and flavones were studied [22–25]. As a continuation of these researches, in the present work, an experimental study on the solubility, solvatochromic effects and preferential solvation of PRX is achieved in single solvents as well as in binary mixture solvents using UV-vis spectroscopy in order to gain insights on the solute–solvent interactions that this drug presents. Also, the thermodynamic parameters involved in the process of solubility, are determined.

# 2 Experimental details

## 2.1 Solvatochromism studies

PRX (CAS 36322-90-4; Molar mass 331.35 g $mol^{-1}$; ≥98%, analytical quality) was purchased from Sigma-Aldrich Chemical Co. USA and was used without further purification. All solvents were HPLC or spectroscopic grade and were used without further purification: *n*-heptane (*n*-Hp ≥ 99.3%), cyclohexane (Cy ≥ 99.0%), carbon tetrachloride ($CCl_4$ ≥ 99.9%), chloroform ($CHCl_3$ ≥ 99.0%), 1,4-dioxane (Diox ≥ 99.0%), acetonitrile (ACN ≥ 99.8%), N,N-dimethylformamide (DMF ≥ 99.8%), dimethylsulfoxide (DMSO ≥ 99.8%), ethyl acetate (EtAcet ≥ 99.8%), 1-octanol (1-OcOH ≥ 99.0%), 1-butanol (1-BuOH ≥ 99.4%), isobutanol (*i*-BuOH ≥ 99.0%), 2-propanol (2-PrOH ≥ 99.7%), 1-propanol (1-PrOH ≥ 99.8%), ethanol (EtOH ≥ 99.9%), methanol (MeOH ≥ 99.8%),

ethylene glycol (Et-Gy ≥ 99.0%), propylene glycol (Pr-Gy ≥ 99.8%) and acetone (Ac ≥ 99.5%). They were obtained from Merck KGaA (Germany). Double-distilled water ($H_2O$) was purified by using a Super Q Millipore System, whose conductivity did not exceed 1.8 μS $cm^{-1}$.

The concentration of the PRX solutions was $8.7 \times 10^{-5}$ M, this concentration was fixed considering getting adequate values in absorbance to minimize the experimental error and that the spectral changes or PRX are concentration dependent [26]. Binary aqueous mixtures were carefully prepared by mass from the corresponding solvents by mixing appropriate volumes of each pure solvent in the following ratios: 1:9, 2:8, 3:7, 4:6, 5:5, 6:4, 7:3, 8:2 and 9:1. All the solutions were obtained by weighting on an analytical balance (Acculab, Sartorius Group) with an accuracy of ±0.0001 g and were stabilized at 25.0 ± 0.1 °C for 10 min.

Optical absorption spectra were recorded using a Cary 50-Varian UV-vis spectrophotometer with thermostatted quartz cells of 1 cm optical path over a wavelength range of the 250–450 nm.

All spectra were determined at 25.0 ± 0.1 °C (temperature control by the Peltier thermostatted cell holders) at the scanning rate of 600 nm $min^{-1}$ and corrected for solvent background by calibrating the instrument to the blank solvent. Each experiment was performed in triplicate and the average value was considered throughout.

## 2.2 Solubility studies

Pure solvents and/or aqueous binary mixtures were prepared in a closed system which provides continuous and stirring thermally conditioned using a stirrer SI Lab Companion 300R. PRX excess was added in a glass tube with a lid of 10 mL capacity containing the pure solvent or the prepared mixtures. A sufficient amount of PRX was added to achieve system saturation. Those systems were held for at least 72 h, with continuous agitation. The saturated system was then analyzed by a UV-Vis spectrophotometer extracting an aliquot of this. The concentrations were determined by the necessary dilutions to the wavelength of maximum absorption of PRX ($\lambda = 329.0$ nm; $\varepsilon = 33\,500$ L $mol^{-1}$ $cm^{-1}$) using methanol as solvent during the dilution process. In order to ensure the reproducibility and saturation of the solutions, all dilutions and solubility measurements were performed in triplicate and experimental results reported were the average of three measurements. Furthermore, a thermodynamic study modifying the temperature systems for water-organic solvent mixtures (EtOH, Et-Gy and Pr-Gy) was carried out at a working temperature (291.15 ± 0.3–307.15 ± 0.3 K).

## 2.3 Data analysis

The data processing and fittings of all equations were carried out using the scientist program Origin v 8.0. Also, for non-linear regression with an iterative procedure, MatLab 2015a program was used. For equation fitting, linear regression was performed by minimal squares. The statistical analysis was performed with IBM SPSS Statistics v 19 program.

# 3 Results and discussion

## 3.1 Analysis in pure solvents

### 3.1.1 Solvatochromism

Solvatochromism of PRX was measured in nonpolar, polar aprotic and polar protic pure solvents. Figure 2 shows as example the electronic absorption spectra of PRX in five representative solvents [27], Cy, EtOH, PrOH, DMSO and $H_2O$.

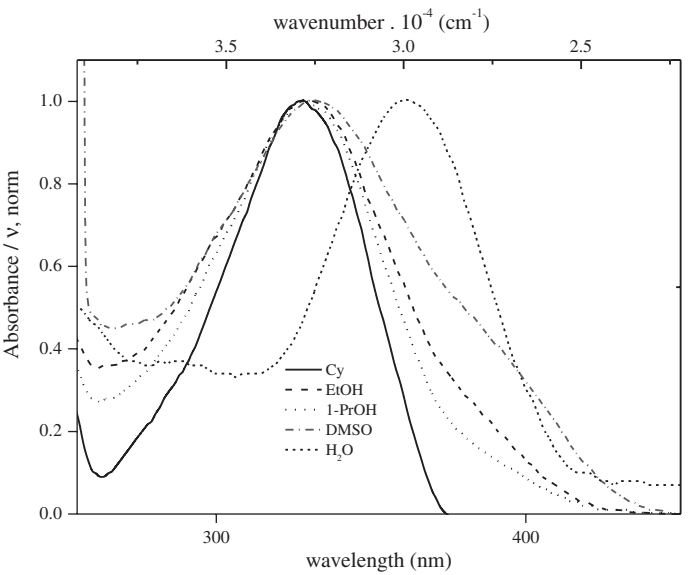


**Fig. 2:** Normalized absorption spectra of PRX in different solvents [27].

In Table 1, the maximum absorption wavelength ($\lambda_{max}$) of PRX in neat solvents along with relevant empirical parameters [28] are summarized. It is well known that molecular structure of PRX exhibits fast tautomeric equilibria presenting various isomers. Furthermore, the existence of intramolecular hydrogen bonds forming six member rings leads to different conformers in the fundamental state. In fact, PRX exists both as a closed and as an open conformer. The presence of the former is favored in apolar solvent. By contrast, in hydrogen-bonding solvents the open conformer prevails [29]. On the other hand, the excited state proton transfer, leading to the interconversion between the keto and enol forms, is also an important feature of PRX [30–32].

The UV-vis absorption spectra of PRX at the present work conditions, exhibit only one band of maximum absorption located in the 324–374 nm range depending on the solvent used. In Cy the maximum absorption is located at 325.0 nm, while in polar protic solvents, a bathochromic shift occurs with increasing the hydrogen bond donor acidity (325.25 nm in 2-PrOH, 326.47 nm in 1-PrOH to 360 nm in $H_2O$). However, this trend cannot be extended to all the analyzed protic solvents, EtOH, Pr-Gy and OcOH present its maxima at 325.72, 327.73 and 327.00 nm respectively. In aprotic solvents, a lower red shift is observed (about 4 nm), being higher when permittivity, the solvent hydrogen-bond acceptor (HBA) capacity as well as, the solvent dipolarity/polarizability increase. While, in no polar solvents a shift to higher wavelengths is noticed when the polarizability increases [*n*-Hp at 325.00 nm ($\pi^*$: 0.08) and $CHCl_3$ at 327.00 nm ($\pi^*$: 0.58)].

The effect of solvent dipolarity/polarizability and hydrogen bonding on the spectral shifts can be interpreted by means of a linear solvation energy relationship (LSER) [33]. Among all the existing solvent polarity scales, in this work, the empirical solvatochromic scale of Kamlet and Taft (KAT) is applied. This treatment uses the following multiparameter equation:

$$\bar{\nu} = \bar{\nu}_0 + s\pi^* + a\alpha + b\beta \tag{1}$$

where $\bar{\nu}$ is the solute maximum absorption wavenumber, $\bar{\nu}_0$ is the value of this property for the same solute in an hypothetical solvent for which $\pi^* = \alpha = \beta = 0$, $\pi^*$ is an index of the solvent dipolarity/polarizability, $\alpha$ is a measure of the solvent hydrogen-bond donor (HBD) capacity, $\beta$ is a measure of the solvent HBA capacity and *s*, *a* and *b* are susceptibility constants.

In order to achieve a better explanation on the solvatochromism of PRX, these solvation parameters were analyzed. Applying Eq. (1) the maximum absorption wavenumbers ($\bar{\nu}_{max}$) of PRX were related to the corresponding solvent parameters $\alpha$, $\beta$ and $\pi^*$ listed in Table 1 and the following multiparametric relationship was obtained:

**Tab. 1:** Maximum absorption wavelength ($\lambda$), wavenumber ($\bar{\nu}$) and solubility (M) of PRX in pure solvents and relevant solvent parameters.

| Solvent | $\lambda$ (nm) | $\bar{\nu}\times10^{-4}$ ($cm^{-1}$) | Solubility$\times10^{3}$ (M) | $\alpha$ | $\beta$ | $\pi^{\star}$ | $\delta^2/1000$ ($J/cm^3$) | Permittivity |
|---|---|---|---|---|---|---|---|---|
| Pr-Gy | 327.73±0.66 | 3.05129 | 1.129 | 1.21 | 0.51 | 0.62 | 0.9165 | 30.2 |
| $H_2O$ | 359.78±0.84 | 2.77945 | 0.01390 | 1.17 | 0.47 | 1.09 | 2.1276 | 78.39 |
| MeOH | 328.46±0.98 | 3.04448 | 1.642 | 0.98 | 0.66 | 0.60 | 0.8797 | 32.70 |
| Et-Gy | 344.68±0.57 | 2.90124 | 0.6866 | 0.90 | 0.52 | 0.92 | 1.0845 | 37.7 |
| EtOH | 325.72±0.75 | 3.07012 | 6.343 | 0.86 | 0.75 | 0.54 | 0.5630 | 24.55 |
| 1-BuOH | 326.51±0.49 | 3.06268 | 1.022 | 0.84 | 0.84 | 0.47 | 0.5333 | 17.51 |
| 1-PrOH | 326.47±1.29 | 3.06304 | 0.9168 | 0.84 | 0.90 | 0.52 | 0.6025 | 20.33 |
| *i*-BuOH | 325.56±0.51 | 3.07167 | 1.373 | 0.79 | 0.84 | 0.40 | 0.4666 | 17.93 |
| OcOH | 327.00±0.10 | 3.05810 | 0.5299 | 0.77 | 0.81 | 0.40 | 0.4439 | 10.30 |
| 2-PrOH | 325.25±0.50 | 3.07456 | 0.6418 | 0.76 | 0.84 | 0.48 | 0.5630 | 19.92 |
| $CHCl_3$ | 327.00±0.15 | 3.05810 | 138.8 | 0.20 | 0.10 | 0.58 | 0.3549 | 4.81 |
| ACN | 324.45±0.98 | 3.08211 | 2.034 | 0.19 | 0.40 | 0.75 | 0.5806 | 37.50 |
| Ac | 327.92±1.24 | 3.04950 | 28.15 | 0.08 | 0.43 | 0.71 | 0.3994 | 20.70 |
| *n*-Hp | 325.00±0.10 | 3.07692 | 0.02565 | 0.00 | 0.00 | −0.08 | 0.0000 | 1.92 |
| Cy | 325.00±0.17 | 3.07692 | 0.1292 | 0.00 | 0.00 | 0.00 | 0.2813 | 2.02 |
| Diox | 326.56±0.38 | 3.06227 | 47.22 | 0.00 | 0.37 | 0.55 | 0.0000 | 2.21 |
| $CCl_4$ | 326.80±0.17 | 3.05998 | 1.149 | 0.00 | 0.10 | 0.28 | 0.2900 | 2.24 |
| DMF | 374.08±0.66 | 2.67322 | 116.0 | 0.00 | 0.69 | 0.88 | 0.6126 | 37.00 |
| DMSO | 328.95±0.30 | 3.03998 | 88.93 | 0.00 | 0.76 | 1.00 | 0.7071 | 46.68 |

$$\bar{\nu} = 30970.1\,(225.1) - 1383.6\,(313.5)\alpha + 1920.0\,(438.6)\beta - 1679.0\,(353.3)\pi^{\star}$$
$$(n=17;\ R^2=0.787;\ \text{Fisher's } F=16.03;\ p\ 0.000118). \quad (2)$$

The values in parentheses are standard errors. Statistical parameters obtained from multiple linear regression analysis result are $R^2$, F and p. In order to consider the validity of LSER results, $R^2$ should be obtained as possible as higher than 0.7. Additionally, p should be derived as having a value close to zero and F with the possible highest value. In this correlation, the maxima absorption wavenumbers determined in DMF and Pr-Gy were no considered due to their anomalous behavior.

The analysis in Eq. (2) reveals that the hydrogen-bond donating power and hydrogen bond accepting strength of the solvent account for 27.8% and 38.5% of the solvent effects on PRX absorption respectively, while solvent polarity accounts for 33.7% of the solvent effects. The selected variables explain the 84.8% of the variability of $\bar{\nu}$, in different solvents.

Figure 3 highlights the fit quality of the full model (Equation 2) by comparing the calculated absorption peak (y-axis) and the measured absorption peak (x-axis) for PRX in the analyzed solvents. As it can be seen from the calculated values achieved with Eq. (2) they are in agreement with the experimental data. The regression coefficients in Eq. (2) are in the order $\beta > \pi^{\star} > \alpha$. This indicates that the hydrogen bonding interactions are responsible for the solvatochromism

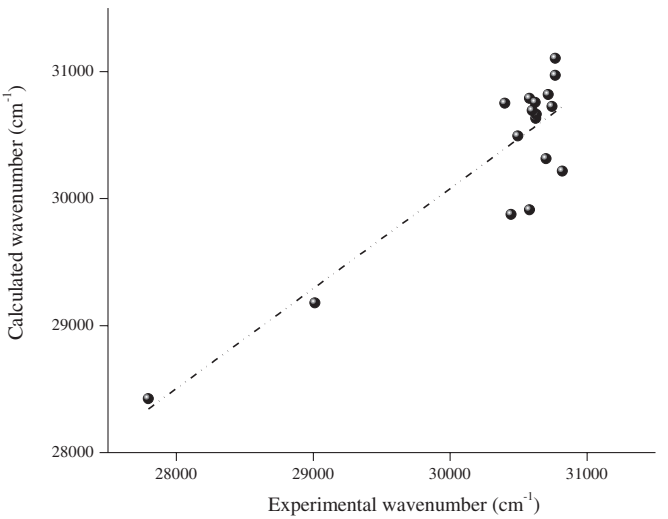


**Fig. 3:** Calculated absorption wavenumbers using KAT equation as a function of the corresponding experimental values for PRX in the analyzed solvents.

observed in the absorption spectra, although the influence of solvent polarity cannot be neglected. The signs of $\beta$ and $\alpha$ coefficients indicate that HBA and HBD solvent characteristics have opposite effects on the position of maximum absorption of PRX. The obtained correlation is different from Andrade and col. results [32]. These authors have analyzed the PRX behavior in 20 protic and aprotic solvents employing a slightly different preparation (seven of them have not been studied in the present work) and obtained that the PRX wavelength was only related to the HBD capacity of the solvents.

While, when solvents with $\alpha \neq 0$ are analyzed, the spectroscopic characteristics of PRX are determined for both non-specific and specific hydrogen bonding solute–solvent interactions. The obtained equation is: $\overline{\nu} = 31006.9\ (356.2) - 1974.8\ (514.6)\ \alpha + 2317.6\ (615.9)\ \beta - 1374.1\ (498.6)\ \pi^*$ ($R^2 = 0.832$). Therefore, the contribution of the parameters $\alpha$, $\beta$ and $\pi^*$ should be considered to explain the solvatochromic effect on PRX. Analyzing the signs of these parameters, specific (HBD) as well as dipolar interactions have the same effects on the position of maximum absorption of PRX. Whereas, for solvents with $\pi^* = 0$, there is no a clear relationship between the wavenumbers of maximum absorption and solvent parameters.

### 3.1.2 Solubility studies

A multiparameter equation describing the process of solubilization was obtained:

$$XYZ = XYZ_0 + \text{energy}_{cf} + \sum \text{energy}_{\text{sto–ste}} \tag{3}$$

In the above equation, $XYZ_0$ is a constant depending only on the solute; $\text{energy}_{cf}$ is the energy for the formation of the cavity where the solute is housed and the term $\text{energy}_{\text{sto–ste}}$ is the sum of all forms of interaction of solute with solvent. To represent the energy required for the formation of the cavity was used as descriptor coefficient Hildebrand and as descriptors of the energies of solute–solvent interaction, the donation ($\alpha$) and acceptance ($\beta$) of hydrogen bonds and polarizability ($\pi^*$) solvents.

Solubility values of PRX (at 298.15 K) in different solvents are shown in Table 1.

Through the statistic program, the coefficients of proportionality for each of these variables were obtained as shown in the following equation:

$$\log S = -2.802 - 0.299\alpha + 0.165\beta + 2.644\pi^* - 2.112(\delta_H^2 / 1000)$$
$$r = 0.734,\ p = 0.0006. \tag{4}$$

It can be seen that the dissolution process is hampered by a significant negative (–2.802) which depends on the intrinsic properties of PRX. Acceptance of

hydrogen bonding solvents and polarizability have a positive effect, while the coefficient of Hildebrand and donating hydrogen bonds have a negative effect. PRX shows higher solubility in $CHCl_3$, Diox, DMF, Ac and DMSO due to high polarizability values and almost null donor hydrogen bonding. PRX has very low solubility in water, due to their high value Hildebrand coefficient.

## 3.2 Analysis in binary mixtures

### 3.2.1 Solvatochromism of PRX

It is known that the behavior of solutes in mixture of solvents is more complex than in pure solvents and the solvation in a mixed solvent system depends on the extent and character of the intra- and intermolecular interactions within the system. Due to these interactions (solute–solvent and/or solvent–solvent interactions), the solute can interact to a greater extent with one of the solvents (preferential solvation). In this kind of mixture the composition of the solvation sphere or cybotactic region is different from the composition of the bulk solvent. In fact, new solvent entities in the solvation shell of the solute molecules with different properties are formed. Instead, in a pure solvent the composition of the solvation sphere of the solute is the same as in the bulk solvent.

When a binary mixture is considered as an ideal one, the maximum absorption wavenumber of the solute should follow a linear additive model according to the following equation [34]:

$$\overline{\nu}_{12\ \text{ideal}} = \overline{\nu}_1 X_1 + \overline{\nu}_2 X_2 \tag{5}$$

where, $X_1$ and $X_2$ are the mole fraction of solvents 1 and 2, and $\overline{\nu}_1$, $\overline{\nu}_2$, $\overline{\nu}_{12}$ are the values of maximum absorption wavenumber of the PRX in the solvent 1, solvent 2 and the binary mixture, respectively.

Mostly due to intermolecular interactions, in the mixed system the liquid components are distributed between two phases (the bulk and the solvation shell of the solute). Thus, the spectral response, $\overline{\nu}_{12}$ in mixed binary solvents is given by a weighted local mole fraction average of the responses $\overline{\nu}_1$ and $\overline{\nu}_2$ for the solute in two pure solvents, expressed by Eq. (6)

$$\overline{\nu}_{12} = \overline{\nu}_1 X_1^L + \overline{\nu}_2 X_2^L \tag{6}$$

where $X_1^L$ and $X_2^L$ depict the mole fraction of the solvents 1 and 2 in the solvation shell respectively. $X_2^L$ can be calculated from experimental measurements through the following expression:

$$X_2^L = \frac{\overline{\nu}_{12} - \overline{\nu}_1}{\overline{\nu}_2 - \overline{\nu}_1} \tag{7}$$

The index of preferential solvation ($\delta_{S2}$) with respect to the solvent 2, can be defined as the difference between $X_2^L$ and $X_2$:

$$\delta_{S2} = X_2^L - X_2 \tag{8}$$

A positive value of $\delta_{S2}$ indicates a preference for solvent 2 over solvent 1, while a negative value of $\delta_{S2}$ signifies vice versa. Seven aqueous mixtures were selected to investigate the effect of solvent composition in the binary systems. In Table 1S and 2S the values of $X_2$, $X_2^L$ and $\delta_{S2}$ for PRX in studied mixtures are shown. In all cases there are deviations from the ideal behavior.

Figure 4, as an example, illustrates the solvatochromic shifts of the absorbance maxima of PRX in $H_2O$-linear alcohols binary mixture as a function of the water mole fraction (solvent 2). With the mole fraction of water in the binary mixture increases, PRX experiences a positive deviation followed by a negative deviation from the ideality. The intersection point between the ideal line and the experimental curves moves to higher water concentration as the length of carbon chain increases (MeOH: 0.31; EtOH: 0.60 and 1-PrOH: 0.756). It is clear, also, that

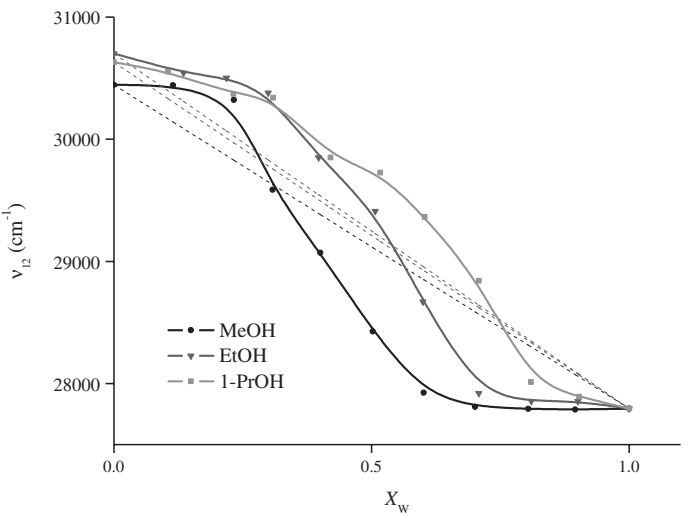


**Fig. 4:** Plot of $\overline{\nu}_{12}$ for PRX in aqueous-linear alcohols mixtures versus the mole fraction of water ($X_w$). (● MeOH, ▼ EtOH, ■ 1-PrOH).

the preferential solvation changes in this point. When the alcohol concentration is higher, PRX is preferentially solvated by this organic solvent. The extension of this preferential solvation is related to the acceptor capacity of hydrogen bond of the alcohol (MeOH: 0.66; EtOH: 0.77 and 1-PrOH: 0.90). But at lower alcohol concentration, water occupies the cybotactic region ($\delta_{S2}$ is positive). PRX could appear in solution as a Lewis acid (owing to its −OH and >NH groups (Figure 1), to establish hydrogen bonds with proton−acceptor functional groups in the solvents (oxygen atoms in −OH or >C=O or −O− groups). However, PRX could also act as a proton−acceptor compound by means of its oxygen atoms in −OH, >C=O, and $-SO_2-$ groups and its nitrogen atoms to interact with hydrogen atoms. Taking account the preferential solvation results, it is possible that at lower water concentration (in alcohol-$H_2O$ mixtures), PRX is acting as Lewis acids with alcohol molecules because this co-solvent is more basic than water, i.e. the Kamlet–Taft hydrogen bond acceptor parameters are $\beta = 0.66$, 0.75 and 0.90 for methanol, ethanol and 1-PrOH respectively and 0.47 for water. On the other region, in water-rich concentration, where $\delta_{S2}$ is positive, this compound are acting mainly as a Lewis base in front to water because the Kamlet–Taft hydrogen bond donor parameters are, $\alpha = 1.17$ for water and 0.98, 0.86 and 0.84 the above mentioned alcohols, respectively.

In 2-PrOH-water mixture, there is evidence that indicates that the proton accepting facility of the oxygen atoms increases in the order primary < secondary < tertiary. On this basis, the hydrogen bond between water and the branched alcohol is more stable than the one between the corresponding normal alcohol and water. Consequently, the number of available water molecules decreases in proportion to the series primary > secondary > tertiary. Therefore, PRX would be rounded preferentially by alcohol molecules ($\delta_{S2}$ negative in all concentrations).

When the aqueous mixtures of non-protic solvents (ACN, DMF and DMSO) are analyzed, in all cases, PRX is preferentially solvated by water in the complete range of mole fractions. It could be explained because PRX is mainly a Lewis base, due to the number of proton-accepting (Lewis base) groups is larger than the number of proton donating (Lewis acid) groups. In $H_2O$-DMSO system, the largest deviations from ideal mixing are observed. Here, the co-solvent presents the biggest values for $\beta$ and $\pi^*$ and $\alpha$ is 0. In so far as, the mixture $H_2O$-DMF presents almost an ideal behavior, its maximum $\delta_{S2}$ is 0.126 ($X_W = 0.847$).

Several non aqueous systems: DMF-1-PrOH, DMF-MeOH and DMF-ACN were also studied (Figure 5). In all of them PRX is preferential solvated by DMF, being the bigger $\delta_{S2}$ for DMF-ACN mixture.

To obtain a quantitative method to evaluate the interactions of PRX in the binary aqueous mixtures, Eq. (1) was used. The values of the Kamlet–Taft

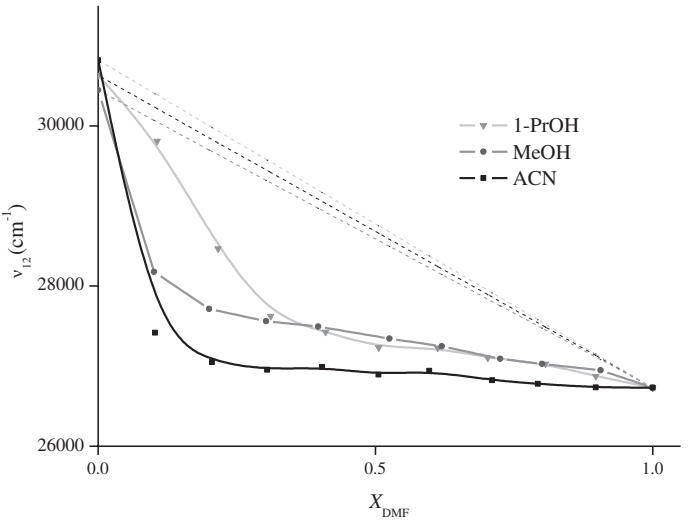


**Fig. 5:** Plot of $\overline{\nu}_{12}$ for PRX versus the mole fraction of DMF ($X_{DMF}$) in binary DMF mixtures. (■ ACN, ● MeOH, ▼ 1-PrOH).

solvatochromic parameters ($\alpha$, $\beta$ and $\pi^*$) for the mixtures were taken from the literature [35] that are in some other percentages of the binary solutions used in this study. So, the reported values of $\alpha$, $\beta$ and $\pi^*$ were separately plotted versus mole fraction of water (or DMF) in order to determine by the fit polynomial, these parameters at the desired mole fraction. In the multiple regressions, the backward selection model was used, which starts with all candidate variables in the model. At each step, the variable that is the least significant is removed. This process continues until only variables with significance remain in the model. Unfortunately, no data were found in the literature for the aqueous solutions of 1-PrOH. The most significant resulting regression equations describing the relationship between $\overline{\nu}_{12}$ and the solvent parameters for PRX are shown in Table 2 (values in parentheses are the respective standard deviations).

Statically, the obtained regression equations demonstrate a very good performance with a squared multiple correlation coefficients ($R^2$) ranged from 0.925 to 0.995, except for the $H_2O$-DMSO and DMF-MeOH mixtures ($R^2 = 0.636$ and 0.800, respectively). According to the obtained results in the aqueous-linear alcohols systems, such as $H_2O$-MeOH and $H_2O$-EtOH an equation containing only the $\pi^*$ parameter shows the best fit. When $H_2O$-2-PrOH is analyzed, the specific solute–solvent associations are present, so the hydrogen bonding interactions are significantly responsible for the solvatochromism observed in the absorption spectra ($\alpha$ and $\beta$ contributions of 37 and 63%, respectively). The

**Tab. 2:** Coefficients of LSER equation for PRX in the binary systems and statistical parameters (values in parentheses are the respective standard deviations).

| System | Parameter | *a* | *b* | *s* | $R^2$ | *F* | p-Value |
|---|---|---|---|---|---|---|---|
| $H_2O$-MeOH | 34233.41 (468.71) | – | – | −5961.46 (509.61) | 0.9383 | 136.84 | 0.000001 |
| $H_2O$-EtOH | 33860.65 (346.09) | – | – | −5490.91 (580.07) | 0.9548 | 190.23 | 0.000001 |
| $H_2O$-2PrOH | −1722.77 (5883.22) | 15108.89 (3529.94) | 25549.25 (3870.39) | – | 0.9812 | 208.33 | 0.000001 |
| $H_2O$-ACN | 32064.77 (339.63) | −3946.99 (396.96) | – | – | 0.9251 | 98.86 | 0.000009 |
| $H_2O$-DMF | 22256.03 (374.07) | 816.33 (115.50) | 2262.16 (436.52) | 3220.41 (186.44) | 0.9955 | 520.59 | <0.0000001 |
| $H_2O$-DMSO | 45987.19 (4468.92) | – | – | −16820.87 (4244.23) | 0.6357 | 15.71 | 0.003288 |
| DMF-MeOH | −3597.3 (14837.83) | – | 67325.04 (25813.88) | −19245.06 (4290.82) | 0.8004 | 14.04 | 0.003552 |
| DMF-1PrOH | 59428.85 (3590.75) | −5096.48 (370.69) | −19178.98 (3619.45) | −19863.86 (1230.36) | 0.9984 | 1302.39 | <0.0000001 |
| DMF-ACN | 57758.72 (3173.15) | −14121.73 (1143.74) | −7836.02 (1152.11) | −27891.16 (4457.68) | 0.9947 | 377.87 | <0.0000001 |

non-protic-aqueous mixtures do not present the same behavior. In $H_2O$-DMSO system, where the solvation preferential index is higher (Table 2) only for intermediate compositions a good correlation between theoretical and experimental values is observed. The multiparametric equation shows that the polarizability plays an important role on PRX solvatochromism. In $H_2O$-DMF system a multiparametric equation displays the best fitted model. In the regression analysis of $\bar{\nu}_{12}$ for this mixture, the hydrogen bonding interactions are as responsible for the solvatochromism observed in the absorption spectra as the nonspecific solute–solvent association caused by dielectric enrichment in the solvent shell (49% for HBA and HBD and 51% for $\pi^*$). Whereas, $H_2O$-ACN mixture, the $\bar{\nu}_{12}$ is only susceptible to the HBD capacity.

The mixtures that include DMF show a different behavior. In DMF-MeOH system which presents the lower squared multiple correlation coefficient, the adjust is good for $0.1 < X_{DMF} < 0.72$ interval. In this mixture, PRX maximum absorption wavenumber is influenced by HBA capacity and polarizability (78% and 22%). According to the obtained results for DMF-1-PrOH and DMF-ACN systems, a multiparametric equation containing $\alpha$, $\beta$ and $\pi^*$ shows the best fit. In both, specific and non-specific interactions have similar contributions. They are $\alpha = 12\%$, $\beta = 43\%$ and $\pi^* = 45\%$ for DMF-1-PrOH and $\alpha = 28\%$, $\beta = 16\%$ and $\pi^* = 56\%$ for DMF-ACN.

In order to achieve a better understanding of the preferential solvation phenomena in the systems, the two-step solvent-exchange model could be applied. Although this model has been mainly applied for solvent mixtures containing hydrogen bond acceptor (solvents with higher $\beta$) and hydrogen bond donor (solvents with higher $\alpha$) solvents [36–38]. The application of this model to other non-aqueous mixtures seems to be also promising [36, 39, 40]. This model was first proposed by Skwierczynski and Connors [37] and further extended by Rosés, Bosch, and co-workers [41, 42].

It suppose that for a binary mixture composed of solvents 1 (S1) and 2 (S2), the $E_T$ value (the solvatochromic property, $E_T = 2.8591 \times 10^{-3}\ \bar{\nu}$, $\text{kcal} \cdot \text{mol}^{-1}$) is an average of the molar transition energies of the absorption maximum of the solute measured in the pure solvents S1 and S2 (with the subscript 2 relating to the most polar component), and in the complex entity S12, that form its solvation microsphere according to their mole fractions within this sphere

$$E_T = X_1 E_{T1} + X_2 E_{T2} + X_{12} E_{T12} \tag{9}$$

where $X_1$, $X_2$ and $X_{12}$ are the mole fractions of S1, S2 and S12 complex, the latter formed by the interaction of solvents S1 and S2, in the microsphere of solvation of the solute (*I*), respectively. $E_{T1}$, $E_{T2}$ and $E_{T12}$ are the molar transition energies of the absorption maximum of the solute, completely solvated by solvents S1, S2 and S12, respectively.

A general model is defined by the following solvent exchange processes

$$I(\mathrm{S1})_m + m\,\mathrm{S2} \Leftrightarrow I(\mathrm{S2})_m + m\,\mathrm{S1}$$

$$I(\mathrm{S1})_m + \frac{m}{2}\mathrm{S2} \Leftrightarrow I(\mathrm{S12})_m + \frac{m}{2}\mathrm{S1}$$

where $I(\mathrm{S1})_m$, $I(\mathrm{S2})_m$ and $I(\mathrm{S12})_m$ represent the solute solvated by S1, S2 and S12, respectively, and $m$ is the number of solvent molecules in the microsphere of solvation of the solute affecting its molar transition energy. These equilibria can be described by two preferential solvation parameters ($f_{2/1}$ and $f_{12/1}$) defined as:

$$f_{2/1} = \frac{X_2^L / X_1^L}{(X_2 / X_1)^m} \tag{10}$$

$$f_{12/1} = \frac{X_{12}^L / X_1^L}{(X_2 / X_1)^m} \tag{11}$$

Mole fractions in the cybotactic region must then be converted into known variables on the basis of preferential solvation parameters, $f$, already defined, considering that the sum of all mole fractions in the cybotactic region and in the solvent's bulk should be equal to one. After making all the mole fraction conversions and the necessary simplifications [43], the following preferential solvation expression is obtained:

$$E_T = \frac{E_{T1}(1-X_2)^m + E_{T2} f_{2/1}(X_2)^m + E_{T12} f_{12/1}(1-X_2)^{\frac{m}{2}} X_2^{\frac{m}{2}}}{(1-X_2)^m + f_{2/1}(X_2)^m + f_{12/1}(1-X_2)^{\frac{m}{2}} X_2^{\frac{m}{2}}} \tag{12}$$

The occurrence of $E_T$ values above or below the value of the solvatochromic properties for the pure components (provided that such variation exceeds experimental uncertainty) points out the presence of significant solvent/solvent interactions and therefore implies a value of $m$ greater than or equal to 2.

The results and some statistical parameters including the $R^2$ coefficient and uncertainty value of each parameter are presented in Table 3.

The results of Table 3 exhibit very good fits of the data for all aqueous binary solvent mixtures except for $H_2O$-DMSO system where the correlation factor is 0.977 and the standard deviation of $E_{T12}$, $f_{2/1}$ and $f_{12/1}$ is very high. In DMF binary systems, although the values of the correlation factors are appropriate, standard deviations of $f_{2/1}$ and $f_{12/1}$ do not. Also, the calculated $E_T$ values for pure solvents are

**Tab. 3:** Preferential solvation parameters of PRX in different binary mixtures.

| System | $m$ | $E_{T1}$ | $E_{T2}$ | $E_{T12}$ | $f_{2/1}$ | $f_{12/1}$ | $f_{12/2}$ [a] | $R^2$ |
|---|---|---|---|---|---|---|---|---|
| $H_2O$-MeOH | 3 | 87.2±0.05 | 79.42±0.27 | 77.9±2.76 | 3.033±0.41 | 0.3054±0.09 | 0.1007 | 0.999 |
| $H_2O$-EtOH | 3 | 87.65±0.26 | 79.51±0.27 | 77.63±7.93 | 0.5063±0.38 | 0.2482±0.21 | 0.4902 | 0.999 |
| $H_2O$-1-PrOH | 2 | 87.54±0.18 | 79.43±0.22 | 76.98±5.28 | 0.2185±0.10 | 0.1563±0.08 | 0.7153 | 0.995 |
| $H_2O$-2-PrOH | 2 | 87.8±0.62 | 79.64±0.62 | 88.97±1.77 | 1.068±2.65 | 2.11±5.73 | 1.9757 | 0.995 |
| $H_2O$-ACN | 2 | 88.02±0.66 | 79.46±0.72 | 78.72±0.67 | 0.008511±0.53 | 1.873±0.77 | 220.0681 | 0.995 |
| $H_2O$-DMF | 2 | 76.53±0.18 | 79.48±0.2 | 79.73±0.26 | 0.02239±0.26 | 1.151±0.38 | 51.4069 | 0.996 |
| $H_2O$-DMSO | 2 | 87.51±1.46 | 79.15±1.09 | 6.2E-6±1500 | 5.555±11.13 | 0.1231±3.05 | 0.0222 | 0.977 |
| DMF-ACN | 2 | 88.12±0.36 | 76.38±0.35 | 76.86±0.81 | 15.9±79.57 | 56.59±30.65 | 3.5591 | 0.998 |
| DMF-1-PrOH | 2 | 87.58±0.75 | 76.81±0.48 | 106.8±52.11 | 75.47±274.33 | 2.598±10.63 | 3.5591 | 0.996 |
| DMF-MeOH | 2 | 87.05±0.27 | 76.46±0.25 | 78.45±0.61 | 9.052±9.8 | 26.32±8.7 | 2.9076 | 0.999 |

[a] $f_{12/2} = \frac{f_{12/1}}{f_{2/1}}$.

in satisfactory agreement with the experimental [average $E_{T_{H_2O}}$ (eq. (12)) = 79.44, experimental $E_{T_{H_2O}} = 79.46$; average $E_{T_{DMF}}$ (eq. (12)) = 76.54, experimental $E_{T_{DMF}} = 76.43$].

Usually, the preferential solvation parameters, $f_{12/1}$ and $f_{2/1}$, determine the tendency of the solute to be more solvated by S12 and S2 than the solvent S1, respectively, and the $f_{12/2}$ parameter measures the preferential solvation of the solute by S12 relative to solvent S2. If $f_{12/1}$ and $f_{12/2}$ are higher than unity it will demonstrate that the solute tends to be solvated by S12 rather than by the pure solvents. The results obtained for PRX show that the $f_{2/1}$ parameter is higher than unity in MeOH and lower than unity in the case of EtOH and 1-PrOH for the studied three systems of aqueous-linear alcohol mixtures, for that in MeOH-$H_2O$ system PRX is more solvated by water. Besides, $f_{2/1}$ and $f_{12/1}$ parameters decrease as the length of the alcohol chain increases. These remarks seem to correspond to the decreasing order of the hydrogen bond donating ($\alpha$) and increasing hydrogen bond accepting ($\beta$) tendencies of the solvents (see Table 1). It should be noted that in these alcoholic mixtures, $E_{T12}$ is close to $E_{T2}$ which indicates the nature of the complex is closer to water than to the respective alcohols. The others aqueous systems (except DMSO-$H_2O$) $f_{12/1}$ and $f_{12/2}$ parameters are higher than unity, so PRX in these mixtures would be more solvated by the solvent complex than the pure solvents. The DMF mixtures exhibit a $f_{2/1} > 1$, so PRX should be more solvated by DMF than the others solvents analyzed. In DMF-ACN mixture, the calculated $E_{T12}$ parameters reflect the interaction of PRX with the mixed entity formed by the ACN with solvent 2 (DMF) and have higher values than those of the pure solvents. This is evidence that this mixture presents a synergistic solvation behavior. This complex could be formed due to both DMF and ACN are dipolar aprotic solvents and are strongly associated.

### 3.2.2 Solubility of PRX. Temperature effects

In order to analyze the process of dissolution, it is possible to consider that it is carried out in a succession of stages: the first step involves the breaking of the existing bonds between adjacent molecules of solute; the second step is the creation of a hole in the solvent to accept the molecule solute. These two steps are produced with consumption of heat and are unfavorable enthalpically, because solute and solvent must beat the cohesive forces that are held together. In the third step, the solute molecule is finally placed in the cavity originated in the solvent. This stage occurs with heat release, enthalpically favorable, due to solute–solvent interactions. The sign and magnitude of $\Delta H°$ for overall processes depend on the nature of these interactions. The entropy is an indicator of the disorder, the more positive the entropy change, the more favorable the process [44].

To minimize errors in the calculation, standard enthalpy and entropy variation for solution process was calculated using the van't Hoff modified equation [45]:

$$-\frac{\Delta H^{\circ}_{\text{Soln}}}{T} = \frac{\delta \ln S}{\delta\left(\frac{1}{T} - \frac{1}{T_{hm}}\right)_p} \tag{13}$$

where $S$ is the solubility in the co-solvent system used, expressed as molar concentration, $R$ represents the gas constant, $\Delta H^{\circ}_{\text{Soln}}$ is the standard change of enthalpy for the solubilization process, $T$ is the absolute temperature ($K$), and $T_{hm}$ is the called harmonic temperature, defined as [46–48]:

$$T_{hm} = \frac{n}{\sum_{n=1}^{n}\left(\frac{1}{T}\right)} \tag{14}$$

The Gibbs free energy change ($\Delta G^{o}$) that takes place during the solubilization process is calculated at $T_{hm}$, considering the approach proposed by Krug et al. [46, 47] using:

$$\Delta G^{\circ}_{\text{Soln}} = -RT_{hm}x(\text{Intercept}) \tag{15}$$

in which, the intercept used is the one obtained in the analysis by treatment of ln $S$ as a function of ($1/T$–$1/T_{hm}$).

The entropy change at $T_{hm}$ for the process under study can be calculated with the equation:

$$\Delta S^{\circ}_{\text{Soln}} = \frac{(\Delta H^{\circ}_{\text{Soln}} - \Delta G^{\circ}_{\text{Soln}})}{T_{hm}} \tag{16}$$

The enthalpy data obtained through the equation (13) are the same to those calculated using the equation of traditional equation of van't Hoff. However, the values of $\Delta G^{\circ}_{\text{Soln}}$ obtained through the equation (15) are slightly different, because in the latter case, it all depends on the solubility data.

The relative contributions of enthalpy ς$H$% and entropy ς$S$% to Gibbs energy of solution process contributions can be calculated with the following equations [49, 50]:

$$\varsigma H\% = \left[\frac{\left|\Delta H^{\circ}_{\text{Soln}}\right|}{\left|\Delta H^{\circ}_{\text{Soln}}\right| + \left|T\Delta S^{\circ}_{\text{Soln}}\right|}\right]100 \tag{17}$$

$$\varsigma S\% = \left[ \frac{\left| T\Delta H^{\circ}_{\text{Soln}} \right|}{\left| \Delta H^{\circ}_{\text{Soln}} \right| + \left| T\Delta S^{\circ}_{\text{Soln}} \right|} \right] 100 \tag{18}$$

In Table 4, the values of the thermodynamic functions and their relative contributions obtained for the systems analyzed are reported. In Figure 6, the graph of enthalpy-entropic compensation for Et-Gy is observed. As it can be seen, the process of dissolution in aqueous binary mixtures of EtOH, Et-Gy and Pr-Gy is not spontaneous in all proportions, but with decreasing $X_W$, the process becomes more spontaneous. For the three co-solvents, the process is endothermic, and a clear trend is not seen by modifying the percentage of organic solvent in the mixture. The entropy change is positive for the three systems studied. It may be noted also that in all cases, the contribution of enthalpy (≅70%) is more important than the entropy contribution to the

**Tab. 4:** Thermodynamic Parameters of solution process.

| Solvent | $X$ | $\Delta H^{\circ}_{\text{Soln}}$ kJ mol$^{-1}$ | $\Delta S^{\circ}_{\text{Soln}}$ J K$^{-1}$ mol$^{-1}$ | $\Delta G^{\circ}_{\text{Soln}}$ kJ mol$^{-1}$ | $\varsigma H$% | $R^2$ |
|---|---|---|---|---|---|---|
| Water | 1 | 57.05 ± 6.99 | 94.27 ± 23 | 28.85 ± 0.13 | 66.92 | 0.934 |
| EtOH | 0.1 | 25.91 ± 4.11 | 6.295 ± 1.39 | 24.02 ± 0.07 | 93.22 | 0.928 |
| | 0.2 | 43.75 ± 3.92 | 70.94 ± 13.4 | 22.52 ± 0.08 | 67.33 | 0.976 |
| | 0.4 | 59.34 ± 4.72 | 136.1 ± 16.1 | 18.64 ± 0.10 | 59.30 | 0.981 |
| | 0.6 | 70.11 ± 15.0 | 174.6 ± 51.2 | 17.89 ± 0.03 | 57.31 | 0.838 |
| | 0.7 | 52.62 ± 4.16 | 119.7 ± 14.2 | 16.80 ± 0.08 | 59.49 | 0.975 |
| | 0.8 | 29.63 ± 3.04 | 48.23 ± 10.3 | 15.14 ± 0.06 | 67.16 | 0.969 |
| | 1.0 | 49.11 ± 8.02 | 110.4 ± 27.4 | 16.01 ± 0.02 | 59.79 | 0.924 |
| Et-Gy | 0.1 | 39.57 ± 4.47 | 48.50 ± 15.2 | 25.07 ± 0.08 | 73.17 | 0.975 |
| | 0.2 | 32.44 ± 3.12 | 29.43 ± 6.36 | 23.64 ± 0.02 | 74.40 | 0.993 |
| | 0.3 | 30.80 ± 3.13 | 31.84 ± 10.6 | 21.28 ± 0.06 | 76.38 | 0.960 |
| | 0.4 | 57.00 ± 6.43 | 125.4 ± 21.9 | 19.48 ± 0.13 | 60.30 | 0.963 |
| | 0.6 | 35.19 ± 5.29 | 54.87 ± 17.9 | 18.72 ± 0.08 | 68.11 | 0.935 |
| | 0.7 | 21.16 ± 7.12 | 11.06 ± 3.40 | 17.85 ± 0.11 | 86.47 | 0.723 |
| | 0.8 | 41.93 ± 4.79 | 82.64 ± 16.3 | 17.25 ± 0.10 | 62.90 | 0.962 |
| | 1.0 | 25.12 ± 2.20 | 29.40 ± 7.51 | 16.32 ± 0.04 | 74.06 | 0.970 |
| Pr-Gy | 0.1 | 19.92 ± 7.39 | −16.49 ± 2.51 | 24.85 ± 0.12 | 80.15 | 0.597 |
| | 0.2 | 20.56 ± 2.67 | −6.28 ± 0.912 | 22.44 ± 0.05 | 91.62 | 0.951 |
| | 0.4 | 35.47 ± 1.02 | 60.38 ± 3.47 | 17.41 ± 0.02 | 66.26 | 0.998 |
| | 0.5 | 33.56 ± 4.82 | 55.89 ± 16.3 | 16.83 ± 0.08 | 66.74 | 0.941 |
| | 0.6 | 25.23 ± 2.04 | 30.15 ± 6.93 | 16.21 ± 0.03 | 73.66 | 0.981 |
| | 0.8 | 12.51 ± 0.69 | 80.46 ± 15.1 | 16.60 ± 0.02 | 80.21 | 0.994 |
| | 1.0 | 32.18 ± 2.38 | 55.32 ± 7.98 | 15.63 ± 0.04 | 66.04 | 0.984 |

$X$, molar fraction.
$\Delta S^{\circ}_{\text{Soln}}$ and $\varsigma H$% calculated with $T_{hm} = 299.15$ K.

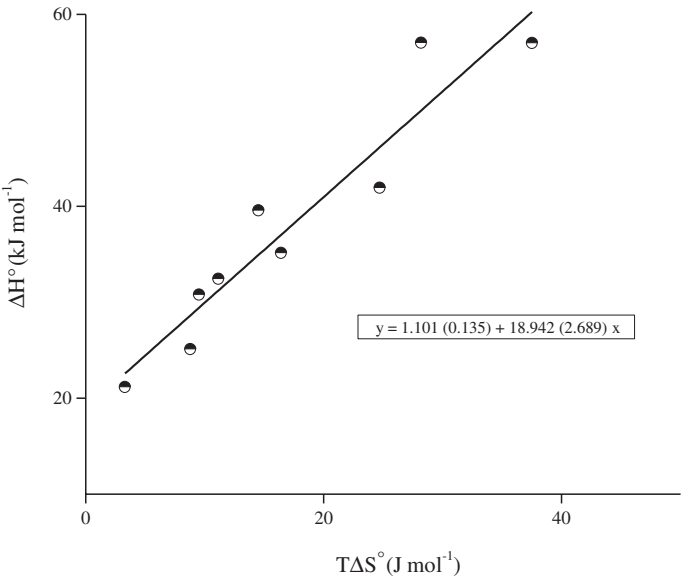


**Fig. 6:** Enthalpy-entropic compensation for PRX in binary mixture Et-Gy-water.

process of solubilization of PRX in the studied mixtures. This is confirmed by values greater than 1 obtained for the $\Delta H°$ vs. $T\Delta S°$ graphs, as it can be seen observed an example in Figure 6.

# 4 Conclusions

The solvent effect on both the electronic absorption spectra and solubility of PRX was analyzed in pure solvents and in binary mixtures by UV-vis spectroscopy.

Linear solvation energy relationships (LSER) were employed to evaluate the solvatochromic shifts observed in pure solvents, using the Kamlet and Taft parameters. The obtained expressions were useful to explore the nature and extension of solute-solvent interactions in aprotic solvents, polar protic solvent and in binary mixtures. The solvatochromism of PRX in pure solvents was determined mainly by specific solute–solvent interactions.

Whilst the PRX solubility depends on the solute–solvent specific interactions, polarizability and the cohesive forces of the solvent, manifested mainly by means of the Hildebrand's solubility parameter. The acceptance of hydrogen bonding solvents and polarizability have a positive effect, while the coefficient of Hildebrand and donating hydrogen bonds have a negative effect on PRX solubility.

For the preferential solvation study, seven aqueous and three DMF binary systems were analyzed. In those mixtures, the local mole fraction, the index of preferential solvation, and exchange constants were calculated. In linear alcohols-$H_2O$ mixtures, PRX is preferentially solvated by alcohol in alcohol-rich mixtures but preferentially solvated by water in water-rich mixtures. These changes occur at higher aqueous molar fraction as the length of the chain of carbons, increases. In 2-PrOH-$H_2O$ solvent, PRX is preferentially solvated by organic molecules. In the rest of aqueous systems, PRX is preferentially solvated by water in the complete range of mole fractions. While, in DMF mixtures, a preferential solvation by DMF, was observed.

The obtained results for aqueous-alcoholic systems show that the $f_{2/1}$ parameter is higher than unity when the co-solvent is MeOH but lower for EtOH and 1-PrOH, for that in MeOH-$H_2O$ system PRX is more solvated by water. Besides, $f_{2/1}$ and $f_{12/1}$ parameters decrease as the length of the alcohol chain increases. Also, in these alcoholic mixtures, $E_{T12}$ is close to $E_{T2}$ which indicates that the nature of the complex is closer to water. The others aqueous systems (except DMSO-$H_2O$) $f_{12/1}$ and $f_{12/2}$ parameters are higher than unity, so PRX in these mixtures would be more solvated by the solvent complex than the pure solvents. DMF mixtures exhibit a $f_{2/1} > 1$, so PRX should be more solvated by DMF than the others solvents analyzed.

The process of dissolution in aqueous binary mixtures of EtOH, Et-Gy and Pr-Gy is not spontaneous, in which the contribution of the enthalpy predominates, in all proportions, but with decreasing $X_W$, the process becomes more spontaneous.

The present work would be a contribution to the knowledge of solvent systems, which would improve the PRX solubilization in the transport process. Also solvation and solubility data presented in this work contribute to expanding the physicochemical information about PRX in neat and binary mixtures.

**Acknowledgments:** Financial support from the National University of San Luis (Argentine Republic) gratefully acknowledged.

## References

1. S. Xu, C. A. Rouzer, L. J. Marnett, Int. Union Biochem. Mol. Biol. **66** (2014) 803.
2. P. Bustamante, M. Peña, J. Barra, Int. J. Pharm. **174** (1998) 141.
3. F. Bouchal, M. Skiba, N. Chaffai, F. Hallouard, S. Fatmi, M. Lahiani-Skiba, Int. J. Pharm. **478** (2015) 625.
4. R. G. Brito, A. A. S. Araújo, J. S. S. Quintans, K. A. Sluka, L. J. Quintans, Expert Opin. Drug Del. **12** (2015) 1677.

5. J. S. Patil, D. V. Kadam, S. C. Marapur, M. V. Kamalapur, Int. J. Pharm. Sci. Rev. Res. **2** (2010) 29.
6. H. Valizadeh, P. Zakeri-Milani, M. Barzegar-Jalali, G. Mohammadi, M. A. Danesh-Bahreini, K. Adibkia, A. Nokhodchi, Drug Dev. Ind. Pharm. **33** (2007) 45.
7. R. G. Sotomayor, A. R. Holguín, A. Romdhani, F. Martınez, A. Jouyban, J Solution Chem. **42** (2013) 358.
8. D. M. Cristancho, A. Jouyban, F. Martínez, J. Mol. Liq. **221** (2016) 72.
9. R. G. Sotomayor, A. R. Holguín, D. M. Cristancho, R. Delgado, F. Martínez, J. Mol. Liq. **180** (2013) 34.
10. S. Vieira Pereira, F. Belotti Colombo, L. A. P. de Freitas, Ultrason. Sonochem. **29** (2016) 461.
11. K. Wu, J. Li, W. Wang, D. A. Winstead, J. Pharm. Sci. **98** (2009) 2422.
12. S. A. Swidan, H. M. Ghonaim, M. M. Ghorab, A. M. Samy, Br. J. Pharm. Res. **3** (2013) 108.
13. A. Karatas, N. Yüksel, T. Baykara, Il Farmaco **60** (2005) 777.
14. A. V. Marenich, C. J. Cramer, D. G. Truhlar, J. Phys. Chem. B **119** (2015) 958.
15. J. P. Graham, M. A. Rauf, S. Hisaindee, M. Nawaz, J. Mol. Struct. **1040** (2013) 1.
16. M. Homocianu, A. Airinei, J. Mol. Liq. **209** (2015) 549.
17. V. Sasirekha, M. Umadevi, V. Ramakrishnan, Spectrochim. Acta, Part A **69** (2008) 148.
18. S. Sanli, Y. Altun, G. Guven, J. Chem. Eng. Data, **59** (2014) 4015.
19. M. Jabbari, J. Mol. Liq. **208** (2015) 5.
20. M. A. Filippa, E. I. Gasull, J. Mol. Liq. **198** (2014) 78.
21. M. A. Filippa, E. I. Gasull, Fluid Phase Equilib. **354** (2013) 185.
22. M. A. Filippa, G. M. Melo, E. I. Gasull, J. Pharm. Chem. Biol. Sci. **3** (2016) 440.
23. M. C. Almandoz, M. I. Sancho, S. E. Blanco, Spectrochim. Acta, Part A **118** (2014) 112.
24. M. C. Almandoz, M. I. Sancho, P. R. Duchowicz, S. E. Blanco, Spectrochim. Acta, Part A **129** (2014) 52.
25. M. I. Sancho, M. C. Almandoz, S. E. Blanco, E. A. Castro, Int. J. Mol. Sci. **12** (2011) 8895.
26. D. Ivanova, V. Deneva, D. Nedeltcheva, F. S. Kamounah, G. Gergov, P. E. Hansen, S. Kawauchi, L. Antonov, RSC Adv. **5** (2015) 31852.
27. G. Angulo, G. Grampp, A. Rosspeintner, Spectrochim. Acta, Part A **65** (2006) 727.
28. Y. Marcus, Chem. Soc. Rev. **22** (1993) 4094.
29. M. Gil, A. Douhal, J. Phys. Chem. A **112** (2008) 8231.
30. J. Bordner, P. D. Hammen, E. B. Whippie, J. Am. Chem. Soc. **111** (1989) 6572.
31. Y. H. Kim, D. W. Cho, S. G. Kang, M. Yoon, D. Kim, J. Lumin. **59** (1994) 209.
32. S. M. Andrade, S. M. B. Costa, Phys. Chem. Chem. Phys. **1** (1999) 4213.
33. M. J. Kamlet, J. M. Abboud, R. W. Taft, Prog. Phys. Org. Chem. **13** (1981) 485.
34. V. Sasirekha, V. Ramakrishnan, Spectrochim. Acta, Part A **70** (2008) 626.
35. Y. Marcus, J. Chem. Soc., Perkin Trans. 2 **8** (1994) 1751.
36. T. Bevilaqua, T. F. Gonçalves, C. G. Venturini, V. G. Machado, Spectrochim. Acta, Part A **65** (2006) 535.
37. R. D. Skwierczynski, K. A. Connors, J. Chem. Soc. Perkin Trans. 2 **2** (1994) 467.
38. M. A. R. Silva, D. C. Silva, V. G. Machado, E. Longhinotti, V. L. A. Frescura, J. Phys. Chem. A **106** (2002) 8820.
39. D. Rácz, M. Nagya, A. Mándi, M. Zsuga, S. Kéki, J. Photochem. Photobiol. A **270** (2013) 19.
40. M. L. Moita, R. A. Teodoro, L. M. Pinheiro, J. Mol. Liq. **136** (2007) 15.
41. M. Rosés, C. Ràfols, J. Ortega, E. Bosch, J. Chem. Soc. Perkin Trans. 2 **8** (1995) 1607.
42. J. Ortega, C. Ràfols, E. Bosch, M. Rosés, J. Chem. Soc. Perkin Trans. 2 **7** (1996) 1497.
43. N. Nunes, C. Ventura, F. Martins, R. E. Leitão, J. Phys. Chem. B **113** (2009) 3071.

44. A. Martin, Physical Pharmacy and Pharmaceutical Sciences, Lippincott Williams & Wilkins, Baltimore, USA (2011), P. 54.
45. D. Pacheco, Y. Manrique, F. Martínez, Fluid Phase Equilib. **262** (2007) 23.
46. R. R. Krug, W. G. Hunter, R. A. Grieger, J. Phys. Chem. **80** (1976) 2335.
47. R. R. Krug, W. G. Hunter, R. A. Grieger, J. Phys. Chem. **80** (1976) 2341.
48. P. Bustamante, J. Pharm. Sci. **87** (1998) 1590.
49. G. L. Perlovich, S. Kurkov, A. Kinchin, AAPS J. **6** (2004) 22.
50. G. L. Perlovich, S. Kurkov, A. Kinchin, A. Bauer-Brandl, Eur. J. Pharm. Biopharm. **57** (2004) 411.

**Supplemental Material:** The online version of this article offers supplementary material (https://doi.org/10.1515/zpch-2017-0946).